



HAL
open science

Sintering of Mass Fractals by Surface Diffusion or by Viscous Flow: Numerical and Scaling Approaches in $d = 2$

Nathalie Olivi-Tran, Romain Thouy, Rémi Jullien

► **To cite this version:**

Nathalie Olivi-Tran, Romain Thouy, Rémi Jullien. Sintering of Mass Fractals by Surface Diffusion or by Viscous Flow: Numerical and Scaling Approaches in $d = 2$. *Journal de Physique I*, 1996, 6 (4), pp.557-574. 10.1051/jp1:1996229 . jpa-00247202

HAL Id: jpa-00247202

<https://hal.science/jpa-00247202>

Submitted on 4 Feb 2008

HAL is a multi-disciplinary open access archive for the deposit and dissemination of scientific research documents, whether they are published or not. The documents may come from teaching and research institutions in France or abroad, or from public or private research centers.

L'archive ouverte pluridisciplinaire **HAL**, est destinée au dépôt et à la diffusion de documents scientifiques de niveau recherche, publiés ou non, émanant des établissements d'enseignement et de recherche français ou étrangers, des laboratoires publics ou privés.

Sintering of Mass Fractals by Surface Diffusion or by Viscous Flow: Numerical and Scaling Approaches in $d = 2$

Nathalie Olivi-Tran, Romain Thouy and Rémi Jullien

Laboratoire de Science des Matériaux Vitreux, Université Montpellier II, Place Eugène Bataillon, 34095 Montpellier, France

(Received 2 November 1995, received in final form 19 December 1995, accepted 21 December 1995)

PACS.61.43.Hv – Fractals: macroscopic aggregates

PACS.64.60.Ak – Renormalization-group, fractal and percolation studies of phase transitions

PACS.81.20.Ev – Powder processing: powder metallurgy, compaction, sintering, mechanical alloying and granulation

Abstract. — Numerical methods are used to model two kinds of sintering processes, by Surface Diffusion (SD) or by Viscous Flow (VF), and are applied to deterministic and random two-dimensional “mass fractals” with various fractal dimensions. In the SD case the relevant partial differential equation is discretized and the evolution of the contour is numerically studied. In the case of viscous flow, a recently introduced approximate “dressing” method is used. In both cases it is shown that the geometrical characteristics which are the perimeter length L , the size ξ and the lower cut-off a , vary as some powers of time t ($L \sim t^{-\alpha}$, $\xi \sim t^{-\beta}$, $a \sim t^\gamma$). The exponents α , β , γ , and their dependence on the fractal dimension D , are estimated from scaling arguments and are found to be different in the SD and VF cases. The SD case is particular in the sense that $\beta \simeq 0$ (no shrinkage) and that, if the initial fractal is too large, it breaks into separate pieces.

1. Introduction

Sintering is an important technological process with applications in many industries (metallurgy, ceramics etc..). It is generally devoted to strengthen a material initially made of a disordered assembly of many components and proceeds by applying temperature and/or pressure [1]. The precise underlying physical mechanisms of sintering depend on the type of materials considered. Here we will focus on materials initially made of aggregated particles, such as silica aerogels, which are highly porous materials of very low density with a huge interface area as revealed by small angle neutron scattering experiments [2–4]. Their structure has been shown to be well described by a random array of fractal aggregates connected together [5]. When such a material is heated during a given time at a temperature smaller than its melting temperature, one observes a net shrinkage and a gradual elimination of the pores as a result of the reduction of the total interface area [6]. On an atomic scale, several physical mechanisms might intervene: i) Evaporation/Deposition (ED), ii) Surface Diffusion (SD), iii) Viscous Flow (VF), but in the case of silica aerogels the two last mechanisms are more likely present with a predominance of VF at higher temperatures [6]. It is only recently that the fractal character

of silica aerogels has been taken into account in a modelization of their sintering process [7–9].

In this paper, our aim is to strengthen the differences between surface diffusion and viscous flow sintering in fractal matter by considering simple examples of two-dimensional fractal shapes. We will consider the regular two-dimensional Vicsek fractal [10] as well as some disordered fractals built with a recently developed method which allows to obtain aggregates of tunable fractal dimension [11]. These are “mass fractals” [12,13] which are here characterized by a given contour (boundary). Our purpose is to study how this contour evolves during sintering. Some characteristics, such as the perimeter length L , the size ξ , and the lower cut-off a are numerically estimated and studied as a function of time t . In both SD and VF cases the total area is constant (due to matter conservation) and all motions of matter are governed by the pressure inhomogeneities due to the changes of curvature along the contour. In both cases the sintering process should end when a circular shape (constant curvature) is reached. The differences come from the nature of the matter transport which is governed by a Fick equation (diffusive transport along the surface) in the SD case [14–16] and a Stokes equation (hydrodynamical transport within the bulk) in the VF case [17–19]. In the SD case the problem reduces to a local partial differential equation for the contour evolution that we solve here numerically using a standard time-space discretization [14]. In the VF case, the problem is much more harder and, except for some two dimensional systems, such as two discs in contact, which can be solved exactly [18], more complex numerical procedures are necessary [19]. Unfortunately they cannot be simply applied to large systems such as the mass fractals considered here. Therefore we have used an approximate “dressing method”, which has been introduced recently [8,9] that we have extended by including the time in an approximate way which is justified *a posteriori*. Therefore, the present treatment of the VF case can be considered as an extension of recent studies [7–9] of the sintering of fractal matter. However, in contrast with these works, we consider here a single fractal shape rather than a collection of connected fractals (which is better suited to model a gel structure).

As a result of the scale invariant properties of the considered fractal shapes, we find that the characteristic lengths, which are the perimeter length L , the size ξ , and the lower cut-off a , vary with time t as power laws, $L \sim t^{-\alpha}$, $\xi \sim t^{-\beta}$, $a \sim t^\gamma$, with exponents α , β , γ , which only depend on the fractal dimension D and that we estimate from scaling arguments in both SD and VF cases. We discuss the special case of surface diffusion for which there is no shrinkage ($\beta \simeq 0$) and for which the material breaks into different pieces if it is originally too large. In Section 2, we present the numerical methods, in Section 3, we give the results and the scaling arguments and in Section 4, we conclude.

2. Principles of the Methods

2.1. GENERATION OF THE INITIAL FRACTAL SHAPES. — Any initial (i.e. non sintered) fractal shape considered here is defined as a contour which is a continuous line drawn around an aggregate built on a square lattice. As a simple example of regular (deterministic) fractal shape, we have considered a Vicsek fractal aggregate [10], which is generated iteratively from a seed particle which is here a square of unit edge length. At the first iteration, four identical squares are stuck to it at distance unity in the four directions (1,0), (0,1), (-1,0), (0,-1) so that we get a cross. At the second iteration, four identical crosses are stuck to it at distance 3 in the same four directions, etc.. (see Fig. 1a). At iteration m , four objects identical to the one obtained at iteration $m - 1$, are stuck at distances 3^{m-1} , so that the Vicsek fractal of the m^{th} iteration contains $M = 5^m$ particles and has a diameter length of $\xi_0 = 3^m$. Therefore the fractal dimension is $D = \log 5 / \log 3 = 1.4649\dots$ Moreover it can be easily shown that its

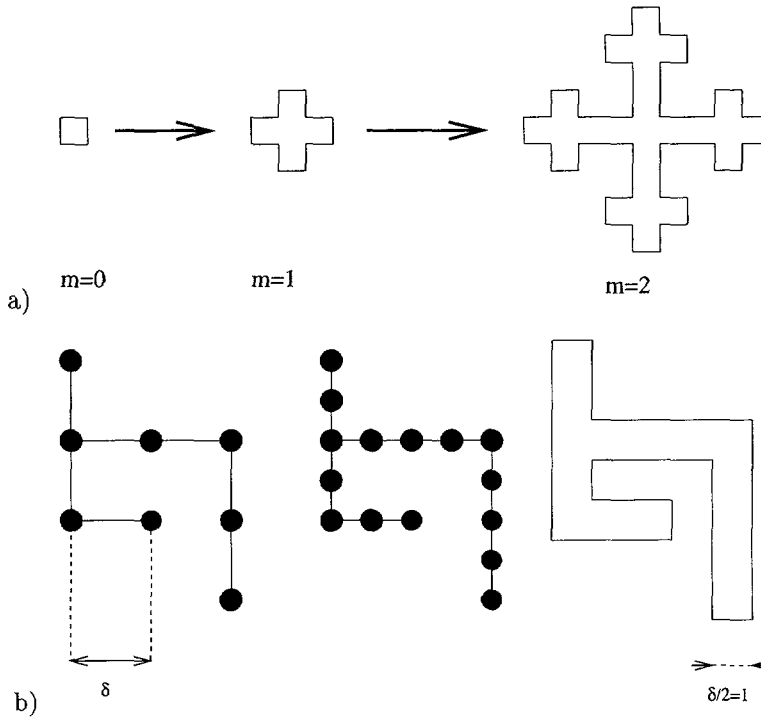


Fig. 1. — Sketch of the procedure used to build the contour of a Vicsek fractal a) and of a disordered fractal b).

perimeter length is $L_0 = 2(5^m + 1)$ and its area A is equal to the number of particles, i.e. $A = M$.

We have also considered random fractal aggregates built with a hierarchical method detailed elsewhere [11]. This method allows to build aggregates on a square lattice with a fractal dimension D given in advance. The idea is to build a new aggregate of 2^m particles by sticking together two aggregates (built independently) of 2^{m-1} particles so that the ratio between their mean quadratic radius of gyration R and the distance between their center of mass Γ fits at best the relation:

$$\Gamma^2 = 4(4^{1/D} - 1)R^2 + \delta^2 \tag{1}$$

where δ is the lattice parameter length. We have considered the version of the algorithm in which only one bond is created when the two clusters are stuck together, so that at iteration m , the aggregate contains $M = 2^m$ particles and $M - 1$ bonds. After that, we have considered a new “decorated” aggregate, in which we have added one particle per bond center and we have defined the initial contour as if all the particles were squares of edge length $\delta/2$, conventionally taken equal to unity in the following (see in Fig. 1b an example with $M = 8$). Therefore the area (=number of particles) of an aggregate of iteration m is $A = 2M - 1 = 2^{m+1} - 1$ and its perimeter length is $L_0 = 2A + 2 = 4M$ but the precise value of the size ξ_0 depend on the generated configuration. The advantage of decorating in such a way the initial aggregate is that we are sure that there are no loops: the whole contour is unique. This is only a technical point which allows to simplify the numerical method to model the sintering process, especially in the SD case (to avoid multiple connected contours).

2.2. SINTERING BY SURFACE DIFFUSION. — In that case, by combining the Fick's law, the linear relation between pressure, curvature and mass conservation, one can obtain the following well-known partial differential equation for the normal displacement z at a given point of the contour defined by its curvilinear abscissa s at time t [14]:

$$\frac{\partial z}{\partial t} = B \frac{\partial^2 K}{\partial s^2} \quad (2)$$

where $K = 1/R$ is the s -dependent local curvature (positive for a tip, negative for a depth) and B is a dimensioned coefficient given by:

$$B = \frac{\ell^4}{t_0} \quad (3)$$

In this expression ℓ is a typical length (of atomic scale) proportional to the diffusion step length and t_0 is a typical time related to the diffusion constant D , the surface tension γ and the temperature T by:

$$t_0 = \frac{kT}{D\gamma} \quad (4)$$

By integrating equation (2) over the contour, it can be shown that the mass(=area) conservation is insured. In the following, the time unit is chosen such that $B = 1$.

The equation (2) is here numerically solved by standard discretisation. Let us assume that at a given time t_i , the contour is represented by a set of N points M_n^i , $n = 1, 2, \dots, N$, and let us define by $\delta_n^i = M_n^i M_{n+1}^i$ (with $N + 1 = 1$) the distances between two successive points. Omitting the time index i , the curvature at point M_n is approximated by:

$$K_n = \frac{2h}{\delta_{n-1}\delta_n} \quad (5)$$

where h is the length of the segment $M_n H$ perpendicular to $M_{n-1} M_{n+1}$ (see Fig. 2a). Then, the first and second derivative of the curvature are approximated by:

$$\frac{\partial K_n}{\partial s} = \frac{K_{n+1} - K_n}{\delta_n} \quad (6)$$

$$\frac{\partial^2 K_n}{\partial s^2} = 2 \frac{\frac{\partial K_n}{\partial s} - \frac{\partial K_{n-1}}{\partial s}}{\delta_{n-1} + \delta_n} \quad (7)$$

This second derivative is used to calculate the new positions M_n^{i+1} at time t_{i+1} , according to:

$$t_{i+1} = t_i + \tau \quad (8)$$

$$h' = h + \tau \frac{\partial^2 K_n}{\partial s^2} \quad (9)$$

The new position M_n^{i+1} is chosen at a distance h' from $M_{n-1}^i M_{n+1}^i$ and at equal distances from M_{n-1}^i and M_{n+1}^i (see Fig. 2a). Note that this procedure insures an automatic homogenisation of the point distribution over the contour.

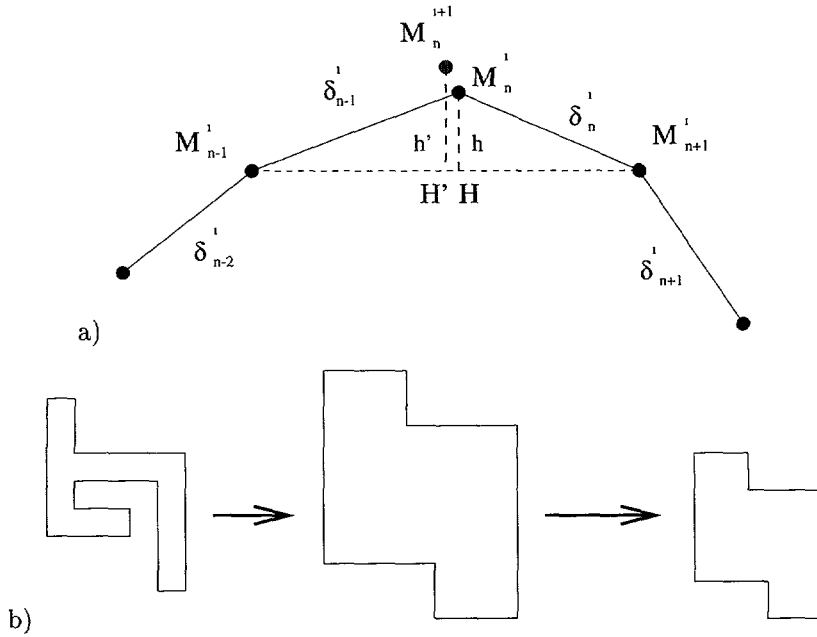


Fig. 2. — Sketch of the discretisation method used for surface diffusion sintering a) and of the dressing method used for viscous flow sintering b).

In order to maintain the error due to time discretisation independent on the length L and the number of points N , we have taken:

$$\tau = C \frac{L^4}{N} \tag{10}$$

where C is a dimensionless constant which controls the errors. The smaller is C , the better is the precision but the longer is the computing time. In the calculations presented below we have taken $C = 10^{-2}$. Note that, correlatively, the larger is the number of points N the smaller are the errors due to space discretisation. Moreover we have checked that the area A (approximated by the surface area of the polygon $M_1 M_2 \dots M_N$) is constant within the uncertainties. In practice, to accelerate the calculation, we reduce N by a factor 2 (by missing one point over 2) when the length L is divided by a factor 2. This trick is very efficient in the cases of fractal shapes for which the initial perimeter length L_0 is very large.

The numerical method has been first checked on an initial contour made of two contacting discs. Starting from a set of a few thousands of points equally distributed over the whole circle, we were able to recover a power-law behavior t^α of the “neck” width with a very low exponent ($\alpha \sim 1/6$) as previously reported (but for two spheres) in the literature [14,20]. When applied to the initial fractal shapes defined above, we were starting with a set of points spaced by unity so that, initially, $N = L_0$. This makes that the initial discretisation is not very smooth. Therefore there may be some errors in the early stage of sintering but, as soon as time goes on, the contour becomes smoother and smoother and these errors disappear.

During sintering, the shape is characterized by its larger and lower cut-off ξ and a . The larger cut-off, which is simply the size, is here approximated by the mean between the height and width of the contour. A natural way to define the lower cut-off a is to relate it to the

inverse of the maximum curvature along the contour at a given time, as it is the typical length associated with the shortest details:

$$a = \frac{2}{K_m} \quad (11)$$

Note that with this definition, the approximation of formula (5) gives $a = \sqrt{2}$, instead of 1, for the non-sintered structure which contains 90° corners. At the end, for a circular shape, ξ and a become equal to each other (circle diameter). Except at the last stage of sintering, the mean curvature \overline{K} over the contour, which is given by:

$$\overline{K} = \frac{1}{L} \oint K ds = \frac{2\pi}{L} \quad (12)$$

(if one assumes no crossing) should be considerably smaller than K_m since $L \gg a$. This is due to the quasi-compensation between tips and depths. Note that the mean curvature would be strictly zero for an open line.

2.3. SINTERING BY VISCOUS FLOW. — In the case of sintering by viscous flow, the entire bulk of the system is generally assumed to be an homogeneous fluid of very high viscosity to which the classical laws of hydrodynamics are applied [21]. For the kind of glassy systems that we are considering, it can be assumed that the convective and gravity forces can be neglected compared to the viscous forces so that the continuity and Navier-Stokes equations reduce to the so-called “Stokes creeping flow” equations [21].

$$\nabla \cdot \mathbf{v} = 0 \quad (13)$$

$$\eta \Delta \mathbf{v} = \nabla p \quad (14)$$

In these equation \mathbf{v} is the velocity field describing the motions of matter, p is the excess of pressure compared to outside, which, as in the preceding section, must be equal to $-\gamma K$ on the boundary, and η is the dynamical viscosity coefficient.

These equation are in general very difficult to handle. In the two-dimensional case that we consider here, Hopper [18] has introduced an exact mathematical treatment based on the use of adequate transformations in the complex plane. He applied his method to the case of two tangent discs but he could not solve more complicated shapes. Van de Vorst *et al.* [19] have introduced some numerical methods able to treat, in principle, any two dimensional contour. However their method becomes time consuming in the case of fractal shapes corresponding to aggregates with many particles as those considered here. More simple approaches, due to Scherer [6], are based on the use of the energy balance of Frenkel [17] (which traduces the fact that the viscous energy loosed by the internal stresses is compensated by the interface energy gained by the reduction of contour perimeter) in combination with some reasonable approximation for the shape evolution. We will use the same kind of method here by considering the approximate dressing procedure which can be considered as an extension of the Scherer's approximate procedure to fractal geometry [8].

Let us assume that the non-sintered aggregate is made of unit squares, as it is the case of all aggregates considered in Section A. The dressing method consists in replacing, at time t , all original squares by larger homotetical ones at the same locations, but with edge length $a_d > 1$ so that some of them may overlap. The area A_d of the dressed structure is calculated numerically and the final sintered shape is obtained after applying an adequate length contraction in order

to insure the mass conservation. Therefore the actual edge length a , which plays the role of the lower cut-off, as in reference [9], becomes:

$$a = \frac{\alpha_d}{f} \quad (15)$$

where f is the length rescaling factor given by:

$$f = \left(\frac{A_d}{A} \right)^{1/2} \quad (16)$$

Also, if one knows the perimeter length of the dressed aggregate L_d , one can calculate the one of the sintered one by:

$$L = \frac{L_d}{f} \quad (17)$$

To simplify the numerical calculation of A_d and L_d , we have limited the a_d values to integers, 1, 2... n ,... so that the dressed aggregate can be put on a grid of unit spacing in order to count the occupied cells and the border unit segments. In Figure 2b, the procedure is sketched on the aggregate of Figure 1b for $n = 2$.

We recall that the physical justification of such a procedure is that the dressing realizes a simple practical way to erase details of small lengths, as in the coarse-graining methods used in the renormalization-group for critical phenomena [22]. Obviously, this is the main effect of the viscous flow which, locally driven by pressure (due to surface tension) tries to erase tips to fill depths. But a non-trivial problem is how to estimate the physical time t . Here we will make the approximation that the actual lower cut-off varies linearly with time according to:

$$a = C \frac{\gamma}{\eta} t \quad (18)$$

where C is a dimension-less constant. In the following we will choose the time units such that $C\gamma = \eta$ and therefore we will have $t = a$. Note that, with this choice, the non-sintered case correspond to $t = 1$ (and not $t = 0$). It is worth noticing that the constant C identifies with the so called *capillary number* which has also been introduced in the context of viscous fingering [23] and which traduces the competition between surface tension and viscous forces.

Formula (18) is supported by the fact that equations (13-14) involve lengths of order a and pressures of order γ/a . Therefore our choice is a direct consequence of a simple scaling analysis of the equations. Obviously, such an approximation is only valid if the scaling holds, i.e. if the sintering process involves several orders of magnitudes. In Section 3.4, this approximation will be justified *a posteriori* by checking the Frenkel's balance. As in all scaling approaches, some details might be forgotten. The precise distribution of the velocity field is ignored. In particular, since we are dressing squares, the final stage of sintering is a square and not a circle and therefore the last stages of sintering will not be well described. In a recent work [24], the two-dimensional Stokes equations have been solved numerically for small disordered chains made of tangent discs and it has been shown that, depending on the initial configuration, some angles between parts of the chain may vary differently during sintering. Also, for multiconnected domain, i.e. objects containing holes, the big holes vanish faster than the small holes [24]. All these effects cannot be reproduced here. However, note that our procedure insures vanishing holes, which is a fundamental aspect of VF sintering compared to SD sintering.

It may be worth noticing that when the dressing method is applied to a couple of tangent discs (by dressing circles and not squares), it gives the well-known \sqrt{t} behavior of the neck width, first found by Frenkel [17], which is only an approximation of the exact singular behavior (which contains logarithmic terms) [18].

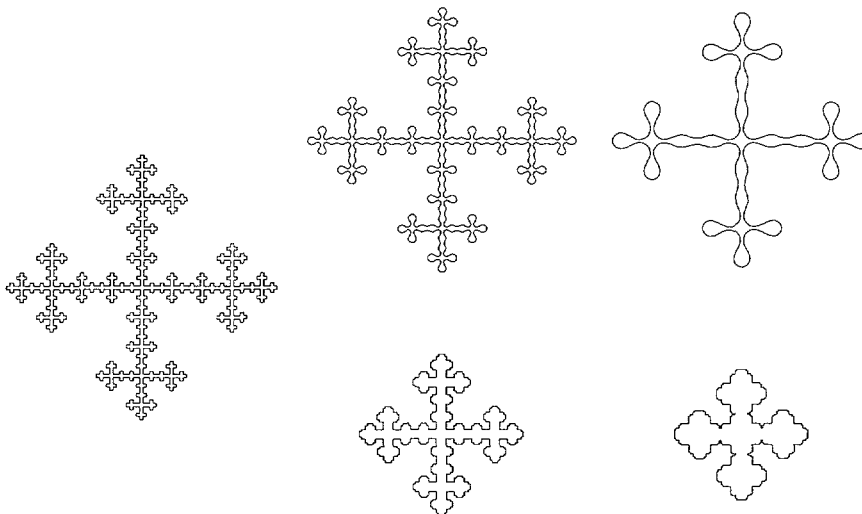


Fig. 3. — Evolution of the contour of a Vicsek fractal containing $M = 3125$ particles in the SD case (top) and in the VF case (bottom).

3. Numerical Results and Scaling Arguments

3.1. GENERAL FEATURES. — To emphasize the qualitative differences between SD and VF cases we first present some pictures for aggregates of modest sizes. In Figure 3, we show how a Vicsek fractal of the fourth generation (containing $5^4=625$ unit squares) is transformed within the two different procedures. One clearly sees that, while there is a gradual shrinkage in the VF case, there is no apparent shrinkage in the SD case (the shrinkage only occurs in the last stage of sintering). As a consequence, while an intermediate shape can be roughly considered as a rescaled version of the original shape in the VF case, this is not true in the SD case: the intermediate shape appears as if the Vicsek fractal would have been made of deformed particles with mean diameters smaller than their nearest neighbor center-to-center distances. Therefore, in the SD case, an intermediate shape cannot be approximated as a self-similar fractal, as there is no longer a unique lowest cut-off. Note that the quantity a , which has been defined by formula (12), corresponds here to the diameter of these pseudo-circular particles. The differences between the VF and SD cases can also be seen in Figures 4, 5 and 6 where we have shown the evolutions of disordered fractals containing $M = 512$ particles with fractal dimensions $D = 1.25, 1.465$ and 1.75 , respectively.

The quantitative results as log-log plots of L , ξ and a versus t are presented in Figures 7, 8 and 9 for disordered fractals of fractal dimensions $D = 1.25, 1.465, 1.75$, respectively. In all cases, we have considered large disordered fractals with $M = 2048$ and the results have been averaged over 7 configurations. In Figure 8, the numerical results for the Vicsek fractal of Figure 3, which has the same fractal dimension, have been superimposed. In the case of the Vicsek fractal one observes some characteristic oscillations with a well-defined period in log-log. These oscillations are due to the so-called lacunarity property of this regular deterministic fractal. The successive abrupt changes in the a values occur when at a given time groups of five pseudo-circles simultaneously merge into a single pseudo-circles of larger radius. Such effects are washed out by randomness in the case of disordered fractals.

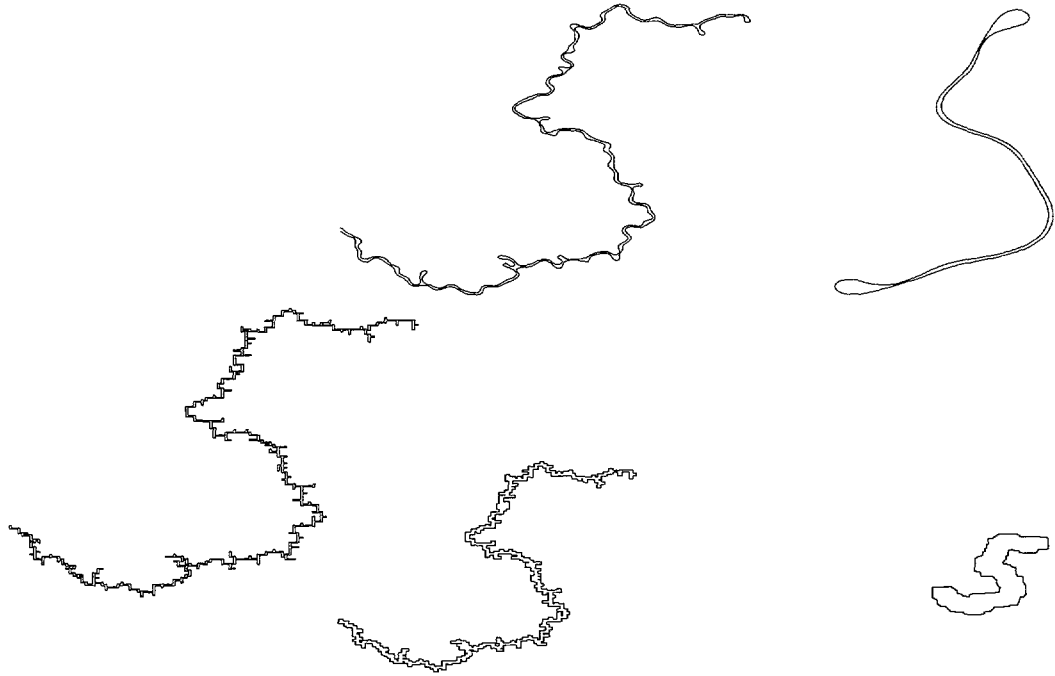


Fig. 4. — Evolution of the contour of a disordered fractal of fractal dimension $D = 1.25$ containing $M = 512$ particles in the SD case (top) and in the VF case (bottom). The times corresponding to the different figures are $t = 0, 5.25, 14180$ in the SD case and $t = 1, 2.46, 36.6$ in the VF case.

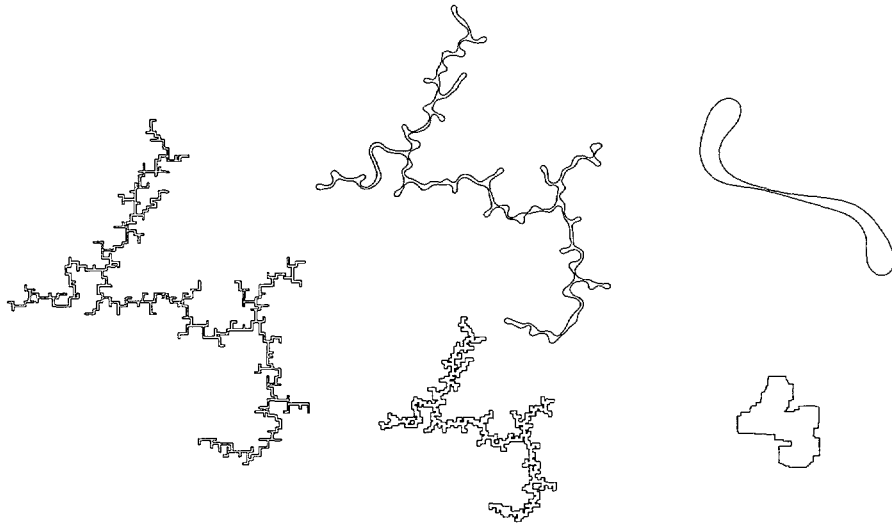


Fig. 5. — Evolution of the contour of a disordered fractal of fractal dimension $D = 1.465$ containing $M = 512$ particles in the SD case (top) and in the VF case (bottom). The times are the same as in Figure 4.

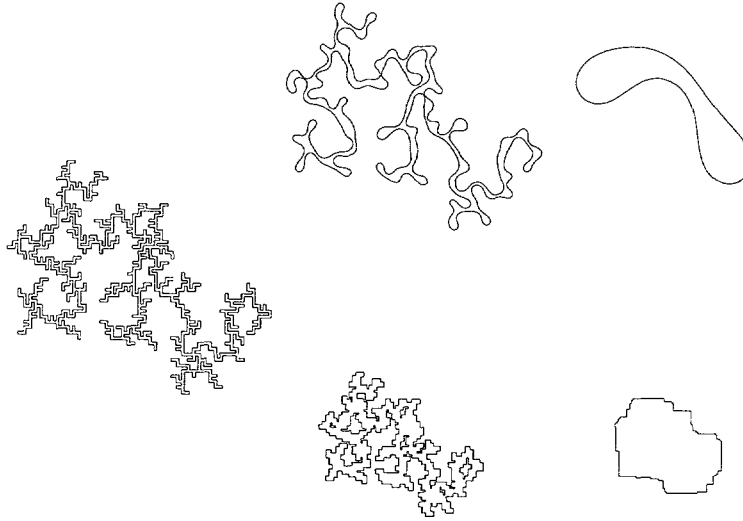


Fig. 6. — Evolution of the contour of a disordered fractal of fractal dimension $D = 1.75$ containing $M = 512$ particles in the SD case (top) and in the VF case (bottom). The times are the same as in Figure 4.

Even if sometimes the linear regimes in log-log are not very well defined, in all the cases we have tried to describe the numerical results by power laws:

$$L \sim t^{-\alpha} \quad (19)$$

$$\xi \sim t^{-\beta} \quad (20)$$

$$a \sim t^{\gamma} \quad (21)$$

The values of α , β and γ can be estimated from scaling arguments.

3.2. SCALING ARGUMENTS. — In the SD case, the exponent γ can be obtained from a trivial scaling analysis of equation (2), assuming that distances of order a and curvatures of order $\frac{1}{a}$ are involved. This gives:

$$\gamma_{\text{SD}} = \frac{1}{4} \quad (22)$$

Our estimation of the other exponents is based on the observation of the behavior in the case of a Vicsek fractal (Fig. 3). Let us make the approximation that a Vicsek fractal containing initially μ^n ($\mu = 5$ here) tangent discs of unit diameter is transformed, after p steps of sintering, into a figure containing μ^{n-p} pseudo-discs of diameter $a \sim \mu^{p/2}$ linked by thin arms of length $\ell \sim \lambda^p$ ($\lambda = 3$ here) and zero width. The scaling of the perimeter length is dominated by the contributions of these arms since $\lambda = 3$ is larger than $\mu^{1/2} = \sqrt{5}$ (in other words $D = \log \mu / \log \lambda < 2$). Since the number of arms scales as μ^{-p} the perimeter should scale as $\left(\frac{\mu}{\lambda}\right)^{-p}$. Using $a \sim \mu^{p/2} \sim t^{1/4}$ and $D = \log \mu / \log \lambda$, this gives:

$$\alpha_{\text{SD}} = \frac{D-1}{2D} \quad (23)$$

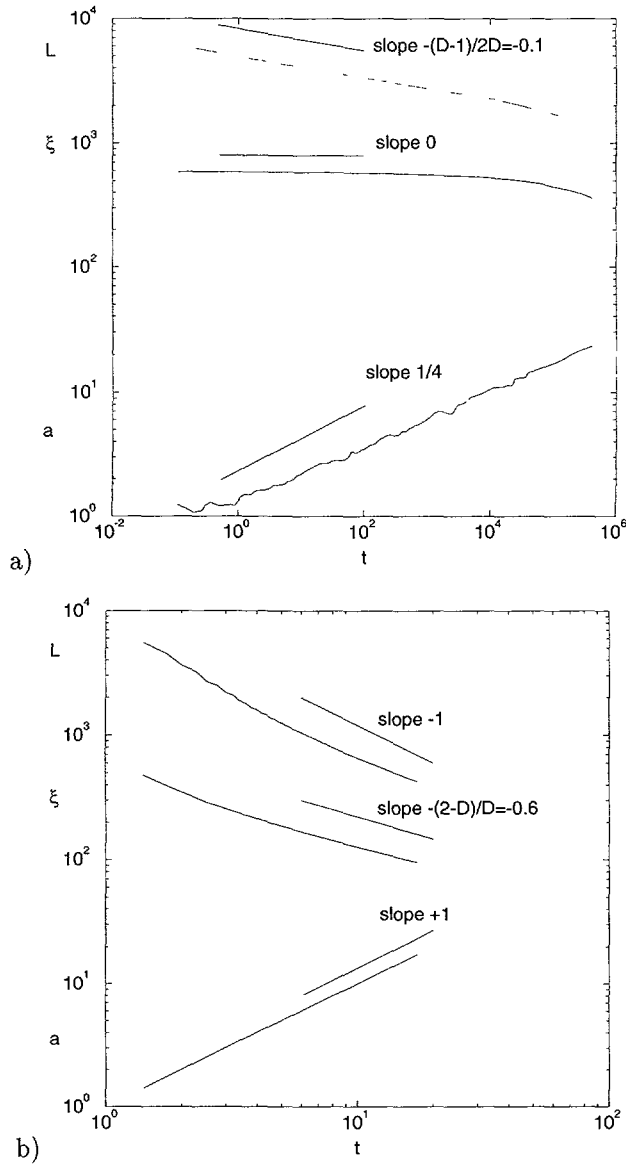


Fig. 7. — Log-log plots of L (top), ξ (middle) and a (bottom) versus t in the case of disordered fractals of fractal dimension $D = 1.25$ containing $M = 2048$ particles in the SD a) and VF b) cases. In both cases the curves result from an average over 7 aggregates and the straight lines correspond to the theoretical slopes expected from scaling arguments.

In this reasoning, the size should decrease with time more slowly than any power law, therefore one should have:

$$\beta_{SD} = 0 \tag{24}$$

The slopes corresponding to the theoretical values of α , β and γ have been indicated in Figures 7a, 8a and 9a. One generally observes a quite good agreement with the numerical results.

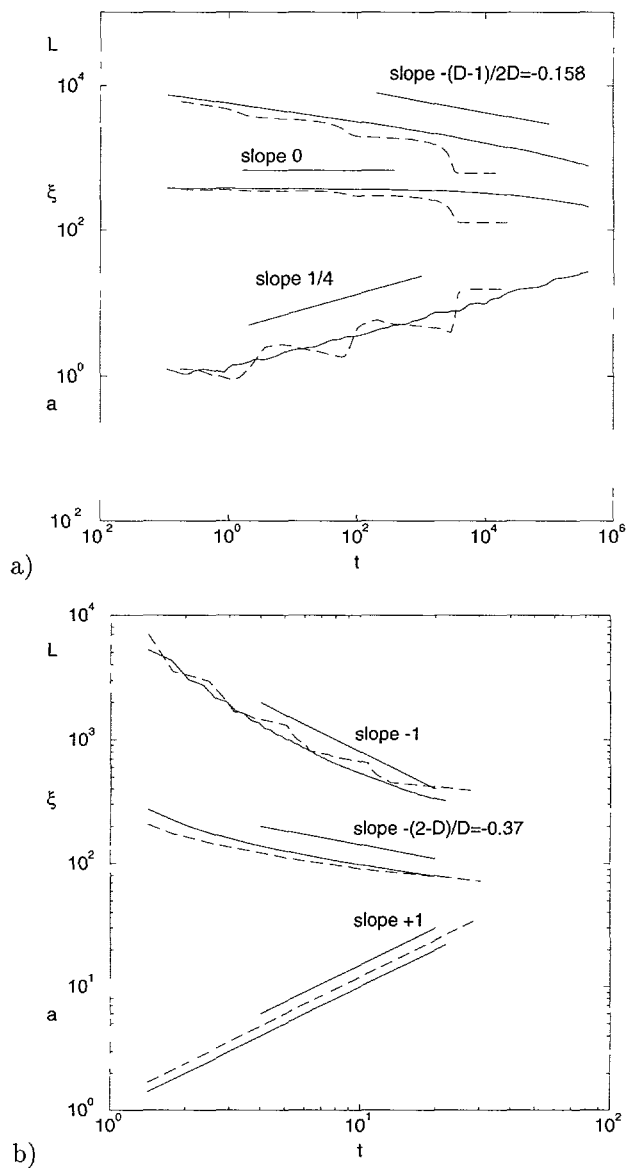


Fig. 8. — Log-log plots of L (top), ξ (middle) and a (bottom) versus t in the case of disordered fractals of fractal dimension $D = 1.465$ containing $M = 2048$ particles in the SD a) and VF b) cases. In both cases the curves result from an average over 7 aggregates and the straight lines correspond to the theoretical slopes expected from scaling arguments. The numerical results for a Vicsek fractal of 3125 particles have been reported on the same figure (dashed curves) with an arbitrary shift in the vertical direction.

In the VF case, we recall that we have postulated, from a scaling analysis of the Stokes equations:

$$\gamma_{VF} = 1 \quad (25)$$

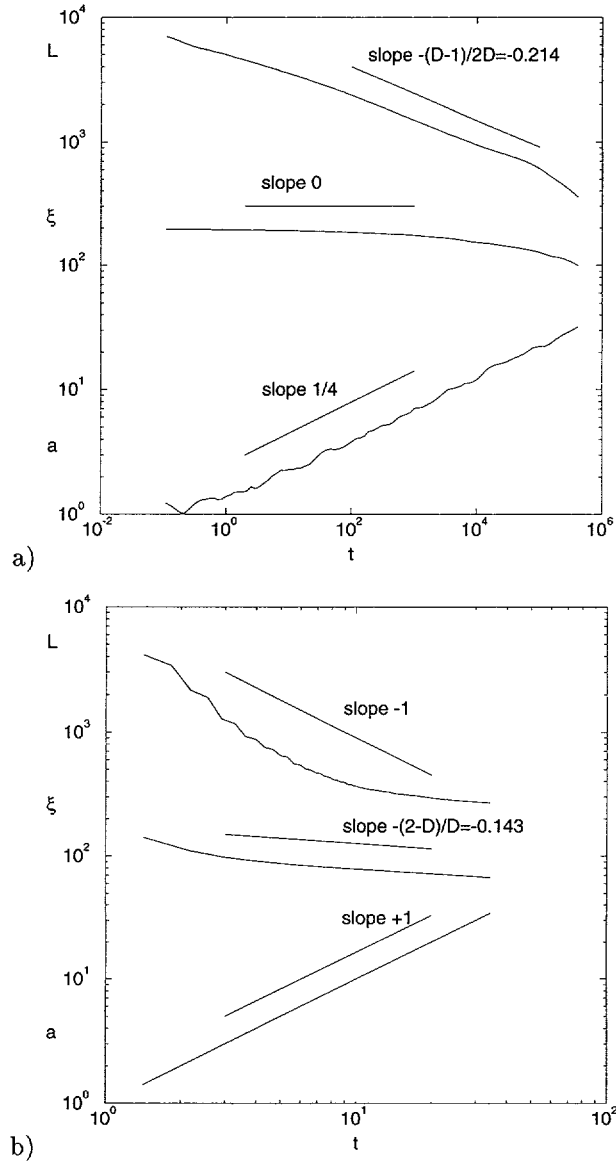


Fig. 9. — Log-log plots of L (top), ξ (middle) and a (bottom) versus t in the case of disordered fractals of fractal dimension $D = 1.75$ containing $M = 2048$ particles in the SD a) and VF b) cases. In both cases the curves result from an average over 7 aggregates and the straight lines correspond to the theoretical slopes expected from scaling arguments.

To obtain the other exponents, we follow (in two dimensions) the scaling reasoning already developed earlier [7]. Here the situation is simpler since, one can assume that, at each stage of sintering, the object remains a mass fractal characterized by the two cut-off ξ and a , the latter being well defined here. Since, from the definition of the Hausdorff fractal dimension [25], the

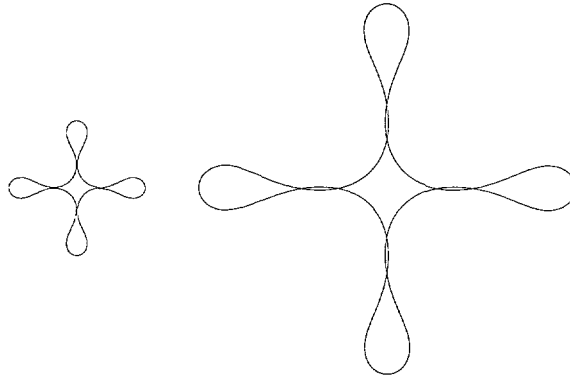


Fig. 10. — Comparison between the SD sintering shapes of Vicsek fractals of the fourth generation at time $t \simeq 400$ and fifth generation at time $t \simeq 20\,000$.

minimum number of discs of diameter a necessary to cover the object is of order $\left(\frac{\xi}{a}\right)^D$, the mass conservation implies $\left(\frac{\xi}{a}\right)^D a^2 = \text{const.}$, and since $a = t$ here, one gets:

$$\beta_{\text{VF}} = \frac{2-D}{D} \quad (26)$$

To estimate the exponent α , the above SD reasoning, with now $\ell = a$, gives $L \sim a^{-1}$, i.e.

$$\alpha_{\text{VF}} = 1 \quad (27)$$

This is in agreement with the hypothesis that the object remains a ramified mass fractal, with well defined arms of thickness a , for which, neglecting vertices and tips, the mass conservation can be simply written $La = \text{const.}$ The slopes corresponding to these theoretical values of α , β and γ have been indicated in Figures 7b, 8b and 9b. Here one observes that the predicted scaling is only verified in the intermediate time regime. There are strong deviations to scaling in the early and last stages of sintering as already observed in previous studies based on the use of dressing method [9]. In particular for large fractal dimensions the $L \sim t^{-1}$ relation is only verified in a very small range of t values as the ramified structure more quickly disappears than for lower fractal dimensions. Also, at small t , the slope of the $\log \xi / \log t$ curves are close to 1, which is the β_{VF} value corresponding to $D = 1$. This is due to our decoration method used to build the initial contour which emphasizes a local linear structure.

3.3. SPLITTING EFFECT IN THE SURFACE DIFFUSION CASE. — We would like to come back to the SD case where some special behavior occurs. In contrast with the VF case, the scaling arguments were developed within very rough assumptions. In particular, in our reasoning based on the analysis of the Vicsek fractal evolution, we approximated the structure by pseudo-discs linked by zero-width arms. In reality these arms become thinner and thinner as the iterations go on so that eventually their thickness changes of sign, i.e. some self-crossings occur, before the end of sintering. This is what happens if one considers the Vicsek fractal of the fifth generation ($M = 3125$) at time $t \simeq 20\,000$ as seen in Figure 10. These crossings should be considered as artifacts of our method. Physically, when the contour starts to meet itself, it

should split into different separate contours which then evolve independently. Therefore if this happens, the sintering process should end with a collection of circles rather than with a unique circle. This fragmentation effect, typical of surface diffusion sintering, was already discussed in the literature for tip shapes with small cone angle [14]. Unfortunately, the self-crossing checks would slow down our numerical procedure considerably and we have not taken care of them. Here we would like to only develop semi-quantitative arguments.

As checked in Figure 10, for a Vicsek fractal of the fifth generation, the sintering process ends with five circles, while for the one of the fourth generation (or any generation below) it ends with only one circle. Therefore the self-crossing event only occurs for initial shapes of sufficiently large mass. To try to get a more quantitative criterion, we have studied the evolution of a dumbbell-like shape made of two circles of diameter d whose centers are separated by a distance H , connected by a thin stick. We have found that a crossing occurs only H/d is larger than a threshold value of order 2.5, almost independently on the stick thickness providing it is sufficiently small. Applied to the Vicsek fractal of the p -th generation, the non-splitting criterion writes $(\lambda/\sqrt{\mu})^{p-1} = (3/\sqrt{5})^{p-1} > 2.5$, i.e. $p \geq 5$, as found here. This reasoning cannot be straightforwardly extended to any fractal dimensions $D = \log \mu / \log \lambda$ as it involves not only exponents but amplitudes. Anyway, in terms of the mass M (number of particles of the original fractal), the non-splitting criterion implies that $M^{\frac{2-D}{2D}}$ should be larger than a non-universal quantity. This means that the fractal shape breaks more easily, i.e. for a lower critical mass, if its fractal dimension is lower. This effect has been checked by our numerical calculations.

It is worth noticing that many self-crossing certainly occurred during the calculations reported in Figures 7a, 8a and 9a, which were performed with quite large initial fractal shapes. We think that taking care of these crossings would have certainly affected the numerical results for ξ , but not too much for L and a .

3.4. FRENKEL BALANCE IN THE VISCOUS FLOW CASE. — In our treatment of viscous flow sintering, the time t does not enter naturally and we have postulated $a \propto t$ from a simple scaling analysis of the Stokes equations. Here we would like to give a justification of this hypothesis by trying to check the Frenkel balance within the framework of the dressing method. In two dimensions the Frenkel balance can be written as follows [6, 17, 21, 22]:

$$2\eta \int \sum_{ij} \dot{\epsilon}_{ij}^2 d\sigma = -\gamma \frac{dL}{dt} \quad (28)$$

where the integral covers the whole area A of the object and where $\dot{\epsilon}_{ij}$ are elements of the rate of deformation tensor:

$$\dot{\epsilon}_{ij} = \frac{1}{2} \left(\frac{\partial v_i}{\partial x_j} + \frac{\partial v_j}{\partial x_i} \right) \quad (29)$$

To make use of our numerical calculations, we express t as a function of a (using relation (18)) and we write the balance between two successive steps (assuming that they are infinitesimally close):

$$2C \int \sum_{ij} \left(\frac{\delta \epsilon_{ij}}{\delta a} \right)^2 d\sigma = -\frac{\delta L}{\delta a} \quad (30)$$

where $\delta \epsilon_{ij}$ is the deformation tensor giving the evolution of the element between the two steps. We recall that C is an unknown dimensionless numerical constant. The main problem is how to

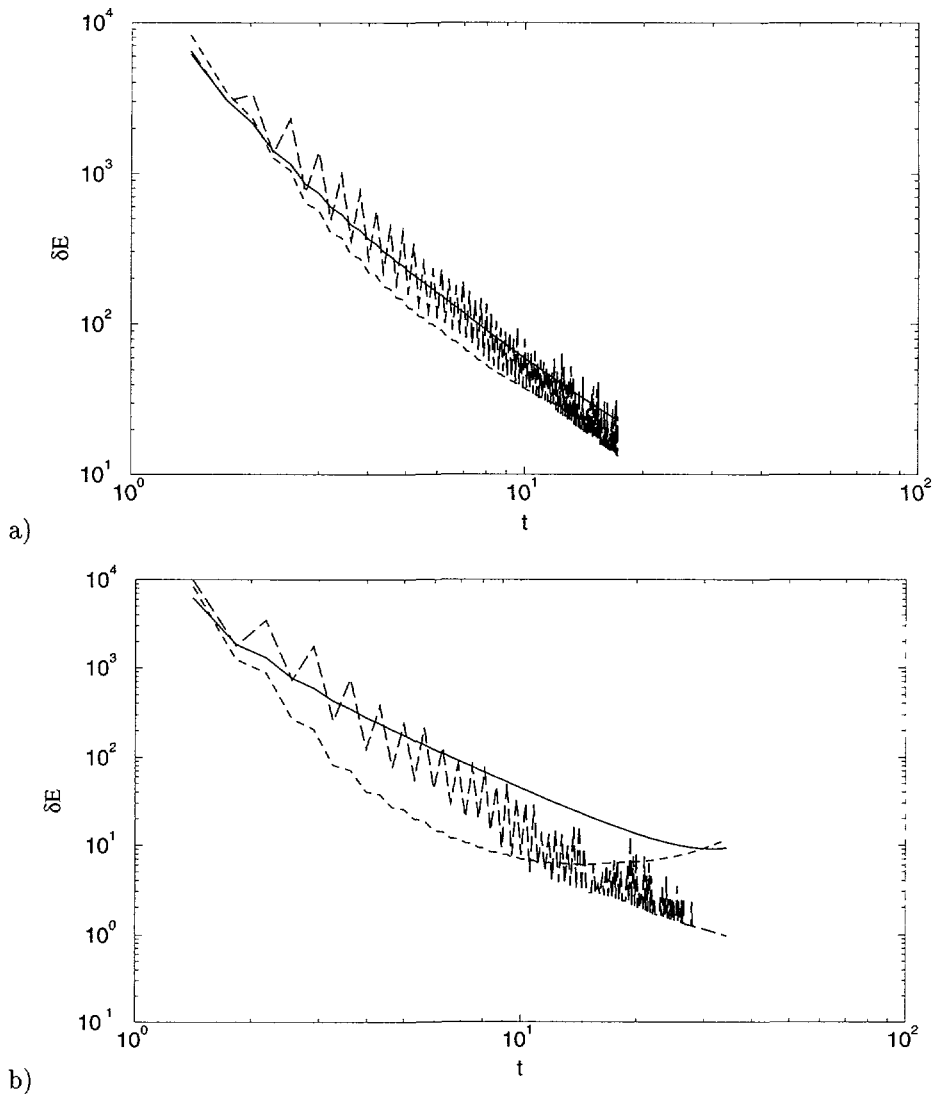


Fig. 11. — Log-log plots of the three quantities δE_{V_1} (solid line), δE_{V_2} (dashed), δE_S (long dashed) as a function of time in the VF case for $D = 1.25$ a) and $D = 1.75$ b).

estimate the viscous energy (proportional to the surface integral) within the dressing scheme. Suppose one deals with a ramified mass fractal for which most of the bulk (except vertices and tips) are arms that can be decomposed in elements of thickness a (= arm thickness) and length ℓ and let us estimate the deformations of this element between two sintering steps. Due to the overlaps the length ℓ stays unchanged after the dressing procedure and its final relative variation is only due to the length rescaling. Therefore, with an adequate choice of axis, $\delta\epsilon_{11} = \frac{\delta\ell}{\ell} = -\frac{\delta f}{f}$ is quantitatively different (and of opposite sign) than $\delta\epsilon_{22} = \frac{\delta a}{a}$ and we can assume $\delta\epsilon_{12} = 0$ (no shear deformation). In this framework the surface integral can be

approximated by:

$$\delta E_{V_1} = \int \sum_{ij} \left(\frac{\delta \epsilon_{ij}}{\delta a} \right)^2 d\sigma \approx A \left(\left(\frac{\delta f}{f \delta a} \right)^2 + \frac{1}{a^2} \right) \quad (31)$$

However these approximations are certainly not valid for later stages of sintering when a well defined bulk is formed. In that case the bulk should be rather decomposed in elements whose lengths, in both directions, have a relative variation of $-\frac{\delta f}{f}$ and therefore the double integral would be better approximated by:

$$\delta E_{V_2} = 2A \left(\frac{\delta f}{f \delta a} \right)^2 \quad (32)$$

We have calculated these two quantities and we have compared them with the right hand term of equation (32) which is proportional to the surface tension energy:

$$\delta E_S = -\frac{\delta L}{\delta a} \quad (33)$$

The results (averaged over 7 samples) are reported as a function of time in Figure 11 for disordered fractals of $M = 2048$ particles with $D = 1.25$ (a) and $D = 1.75$ (b). Despite the odd-even oscillations which are due to our discretisation, the E_S curve follows remarkably the E_{V_1} curve (and scales as t^{-2} as predicted) during most of the sintering process, except at a given stage where it starts to pass below it and reach the E_{V_2} curve. For $D = 1.75$, the crossover occurs earlier than for $D = 1.25$. This is reasonable since for larger fractal dimensions the ramified structure is loosed much more quickly. This check gives a strong support to our hypothesis $t \propto a$. Moreover it allows to estimate $C \approx 0.5$. Note however that the coincidence between the E_S and E_{V_2} curves is not permanent and E_S becomes quantitatively different from E_{V_2} at the very end of the sintering process. But it was clear from the beginning that the dressing method could not model reasonably this regime. It is obvious that a precise knowledge of the velocity field is necessary to know how an object looses the memory of its original shape to finally reach a perfect circle.

4. Conclusion

We have found that the time evolution of a two-dimensional fractal shape under sintering is completely different if the sintering is due to surface diffusion or to viscous flow. In particular the shrinkage is considerably lower in the SD case as the size ξ decreases more slowly than any power law of time. Moreover, if the initial fractal is too large it breaks into separate pieces. At this stage, our calculations are restricted to two dimensions and it is difficult to make any quantitative comparison with experiments. However the scaling reasonings can be simply extended to three dimensions and the expressions for the exponents can be translated by straightforwardly replacing the space dimension 2 by 3 in their expressions as a function of D . When extending to three dimensions and comparing with experiments, it should be remembered that L becomes the internal surface area, which is available in many experiments, such as gas adsorption, and ξ and a are the limits of the fractal scaling, as they can be seen in Small Angle Neutron Scattering (SANS) experiments. Also, if the structure made of connected fractals is preserved, the density ρ should scale as ξ^{-3} . In the case of the viscous sintering of silica aerogels, many quantitative comparisons between experiments and theoretical results

based on the dressing methods have already been done [7,9]. It would be interesting to perform the same kind of comparisons in the case of sintering by surface diffusion. Recently some sintering experiments have been done by the Montpellier's group on silica aerogels at much smaller temperatures than before [26]. Therefore, in that case, one can hope that sintering by surface diffusion occurs in a larger range of time allowing a possibility to test the scaling laws obtained here. We hope to have SANS data soon available to perform some quantitative comparisons in a forthcoming publication.

Acknowledgments

We acknowledge interesting discussions with J. Phalippou, T. Woignier and G. Cohen-Solal. Calculations were done on the computers of the CNUSC (Centre National Universitaire Sud de Calcul), Montpellier (France).

References

- [1] Brinker C.J. and Scherer G.W., Sol-gel science: the physics and chemistry of sol-gel processing (Academic Press, London, 1990).
- [2] Schaefer D.W., Martin J.E. and Keefer K.D., *Phys. Rev. Lett.* **56** (1986) 2199.
- [3] Freltoft T., Kjems J.K. and Sinha S.K., *Phys. Rev. B* **33** (1986) 269.
- [4] Vacher R., Woignier T., Pelous J. and Courtens E., *Phys. Rev. B* **37** (1988) 6500.
- [5] Hasmy A., Anglaret E., Foret M., Pelous J. and Jullien R., *Phys. Rev. B* **50** (1994) 6016.
- [6] Scherer G.W., *J. Am. Ceram. Soc.* **60** (1977) 236; **60** (1977) 243; **74** (1991) 1523.
- [7] Sempéré R., Bourret D., Woignier T., Phalippou J. and Jullien R., *Phys. Rev. Lett.* **71** (1993) 3307.
- [8] Olivı-Tran N., Jullien R. and Cohen-Solal G., *Europhys. Lett.* **30** (1995) 393.
- [9] Olivı-Tran N. and Jullien R., *Phys. Rev. B* **52** (1995) 258.
- [10] Vicsek T., *J. Phys. A* **16** (1983) L647.
- [11] Thouy R. and Jullien R., *J. Phys. A* **9** (1994) 2953.
- [12] Jullien R. and Botet R., Aggregation and fractal aggregates (World Scientific, Singapore, 1987).
- [13] Feder J., Fractals (Plenum, New York, 1988).
- [14] Nichols F.A. and Mullins W.W., *J. Appl. Phys.* **36** (1965) 1826.
- [15] German R.M. and Lathrop J.F., *J. Mater. Sci.* **13** (1978) 921.
- [16] Carrol D.R. and Rahaman M.N., *J. Europ. Ceram. Soc.* **14** (1994) 473.
- [17] Frenkel J., *J. Phys. (Moscow)* **9** (1945) 385.
- [18] Hopper R.W., *J. Fluid Mech.* **213** (1990) 349; **230** (1991) 355; **243**(1992) 171.
- [19] van de Vorst G.A.L. and Mathieu R.M.N., *J. Comput. Phys.* **100** (1992) 50.
- [20] Kuckzynski G.C., *Trans AIME* **185** (1949) 169.
- [21] Batchelor G.K., An introduction to fluid dynamics (University Press, Cambridge, 1967).
- [22] Pfeuty P. and Toulouse G., Introduction to the renormalization-group and critical phenomena (Wiley and sons, New York, 1977).
- [23] Ben Amar M., Combescot R. and Couder Y., *Phys. Rev. Lett.* **70** (1993) 3047.
- [24] van de Vorst G.A.L., Modelling and numerical simulation of viscous sintering, PhD thesis (Eindhoven University of Technology, The Netherlands, 1994).
- [25] Mandelbrot B.B., The fractal geometry of nature (Freeman, San Francisco, 1982).
- [26] Woignier T., private communication.